Mechatronics 24 (2014) 1–11

Contents lists available at ScienceDirect

Mechatronics

journal homepage: www.elsevier.com/locate/mechatronics

Extended and reduced POG dynamic model of an automatic corking machine for threaded plastic caps

R. Zanasi [a], F. Grossi [a,*], N. Giuliani [b]

[a] Department of Engineering "Enzo Ferrari", University of Modena and Reggio Emilia, Modena, Italy
[b] Tissue Machinery Company S.p.A., Granarolo dell'Emilia, BO, Italy

ARTICLE INFO

Article history:
Received 24 May 2013
Accepted 15 November 2013
Available online 19 December 2013

Keywords:
Dynamic modeling
Power-Oriented Graphs
State space transformation
Model reduction

ABSTRACT

The aim of this work is to show how the modeling of an electromechanical system can be addressed using the energy-based graphical modeling technique named "Power-Oriented Graphs" (POG). Differences and analogies of POG against Bond Graphs modeling technique are discussed. The paper presents the POG dynamic model of an automatic corking machine for threaded plastic caps: the system is composed by two electric motors moving a ball screw/spline that realizes the linear/rotary motion necessary to screw a plastic cap on a bottle. First an extended POG model is presented, together with the equivalent Bond Graph model, then some proper congruent state space transformations and a POG-based graphical method are introduced to transform and reduce the system dynamic model. Simulation and experimental results are finally presented and compared.

1. Introduction

The choice of a modeling technique is a very important issue when dealing with the modeling of dynamic physical systems. Many graphical modeling techniques that use an energy-based approach have been introduced in the past years: the Bond Graphs (BG) [1,2], the Power-Oriented Graphs (POG) [3], the Energetic Macroscopic Representation (EMR) [5], etc. The basic concept of all these techniques is the use of an energy-based approach which clearly shows how the power flows within the system. Some comparisons among these techniques can be found in [6,7]. In [8] a combination of BG and standard block diagrams is used to represent mechatronic systems in a holistic modeling approach. Traditionally these techniques have been developed to model systems in the electric, mechanical and hydraulic domains, but in last years BG are extending their modeling capabilities also to the chemical and thermodynamic field, see [9] and to the modeling of measurement uncertainties in electromechanical applications, see [10]. In this work the POG modeling technique is first introduced and compared with BG and then exploited to model the system. The POG technique is based on a modular structure which allows to obtain the model of a complex physical system by interconnecting the POG models of all its subsystems interacting each other through their power ports. The POG block schemes are easy to draw and read even for beginners, they are in direct correspondence with the state space dynamic equations of the system, they are very compact (use vectorial notation), they guarantee energy conservation, they allow to transform (reduce and/or invert) dynamical systems and they can be directly translated into Simulink for simulations.

The problem of model order reduction is under investigation since many years with several approaches, see [11] and the references therein. In particular, in model order reduction of physical systems, preservation of passivity in the reduced model is a crucial issue and some approaches are introduced in [11–13]. The POG approach allows to transform and reduce models, preserving the system properties, when some dynamic elements of the system tend to zero or to infinity, see [14]. Moreover, in this paper two methods to obtain an input–output static model by reducing a dynamic model are introduced: one based on POG state-space representation and the other based on POG graphical scheme.

An example of dynamic modeling of a system with belt transmission and screw ball is given in [15] where Lagrange method is exploited to write the equations of the system. Another example of modeling of a ball-screw driven servomechanisms, to obtain a design methodology, is presented in [16,17]: here the modeling is in part addressed using non-structured standard block schemes as opposite to POG block schemes for which many structural properties hold (such dissipativity, power sections, etc.) as it will be discussed in the paper. In this paper the mechatronic system presented in [18] (automatic corking machine for threaded plastic caps with a ball screw/spline) is considered and modeled exploiting the POG approach.

* Corresponding author. Tel.: +39 0592056333.
E-mail addresses: roberto.zanasi@unimore.it (R. Zanasi), federica.grossi@unimore.it (F. Grossi), ngiuliani@tissue.it (N. Giuliani).

0957-4158/$ - see front matter © 2013 Elsevier Ltd. All rights reserved.
http://dx.doi.org/10.1016/j.mechatronics.2013.11.002

The corking machine here considered is an electromechanical system with two degrees of freedom: two controlled electrical motors move a ball screw/spline that actuates the linear-rotary motion necessary to screw a plastic cap on a bottle. A prototype of the machine has been realized. The paper presents an extended dynamic model of the whole machine and then introduces some POG-based transformation techniques in order to obtain the transformed and reduced model. An accurate dynamic modeling of the whole system is very useful in the design of the machine (model-based design) because it provides information for the choice of parameters, the evaluation of performances that can be obtained and the design of the control. The simulation model allows the test of different control algorithms in simulation before the implementation on the real machine.

2. Graphical energy-based modeling techniques

In this section the basic properties of the Power-Oriented Graphs technique are presented and a comparison with the well-known Bond-Graphs is given. Both techniques are graphical approaches to the modeling of dynamic systems and they are energy-based: the components interact through energy ports and the power flowing through these ports is clearly shown in the graphical representation. This *energetic approach* is useful for modeling because all the dissipative physical systems are characterized by these properties: (1) a physical system always *stores and/or dissipates energy*; (2) the dynamic model of a physical system describes *how the energy moves* within the system, (3) the energy moves from point to point only by means of two *power variables*. The product of the two power variables in each physical domain (electric, mechanical and hydraulic) is power. In BG the power variables are defined as *effort* and *flow*, see for instance [24], while in POG the *across* and *through* variables,[1] see [4], are used as shown in Fig. 1. For the sake of simplicity, in the following e will denote effort and across variables, while f will denote flow and through variables thus considering only the POG-BG analogy in the electric and hydraulic domains.

The Bond Graphs technique is well-known and well established, therefore it will not be described in details in the paper but only the issues useful for a comparison with POG will be considered. In the Bond Graphs representation a half arrow represents a "power bond" where the effort and flow variables are written respectively above and below the half arrow:

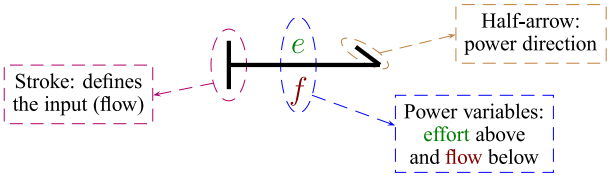

The direction of the half arrow defines the direction of positive power transport. The vertical stroke defines the input variable of the corresponding mathematical model: when the stroke is at the begin of the half-arrow the input variable is the *flow*, when the stroke is at the end of the half-arrow the input variable is the *effort*. The following *nine basic node-types* are distinguished in BG:

– 1-port components: C, I, R, Se, Sf

[1] An *across* variable is a variable defined between two points (i.e. voltage, speed, pressure), a *through* variable is a variable defined in each point of the space (i.e. current, force, flow rate).

	Variable	Electrical	Mech. Trans.	Mech. Rot.	Hydraulic
BG	**Effort:** e	V Voltage	F Force	τ Torque	P Pressure
	Flow: f	I Current	v Velocity	ω Angular Vel.	Q Flow Rate
POG	**Across:** v_e	V Voltage	v Velocity	ω Angular Vel.	P Pressure
	Through: v_f	I Current	F Force	τ Torque	Q Flow Rate

Fig. 1. Bond Graphs definitions of the *effort* and *flow* variables and Power-Oriented Graphs definitions of*across* and *through* variables.

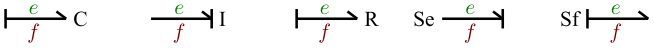

represent physical elements that store or dissipate energy (such as capacitor, inductor, resistor) or sources (such as voltage or current sources).

– 2-port components: transformer TF and gyrator GY

represent physical elements that transform the power without storing nor dissipating energy (such as transformers, gear reduction). A letter M can also appear in the node symbol, MTF and MGY, standing for "modulated", thus expressing that the 2-port component depends on an external modulating signal.

– 3-port components: 1-junction and 0-junction

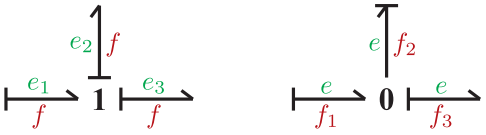

represent connections: the 1-junction connects elements sharing the same flow (i.e. the series connection in the electric domain), the 0-junction connects elements sharing the same effort (i.e. the parallel connection in the electric domain). Note that the number of ports in junctions is not limited to 3 thus allowing to connect in general n elements.

2.1. The Power-Oriented Graphs technique

The main features of the POG modeling technique are stated in [3]. The POG technique uses only the two basic blocks shown in Fig. 2 for modeling physical systems:

(a) The ***elaboration block*** (e.b.) is used for modeling all physical elements that store and/or dissipate energy (i.e. spring, mass, damper, capacitor, inductor, resistor, etc.). With this block it is possible to model the 1-port elements of types C, I, R used in the BG technique. The summation element at the top of the block is suitable for modeling all the 3-port connection elements (0-junction and 1-junction) of the BG technique. The black spot within the summation element represents a minus sign that multiplies the entering variable. The e.b. can be scalar or vectorial and for linear systems matrix $\mathbf{G}(s)$ is always a square matrix of positive real transfer functions.

(b) The ***connection block*** (c.b.) is used for modeling all physical elements that "transform the power without losses" (i.e. *neutral elements* such as gear reductions, transformers, etc.). This block

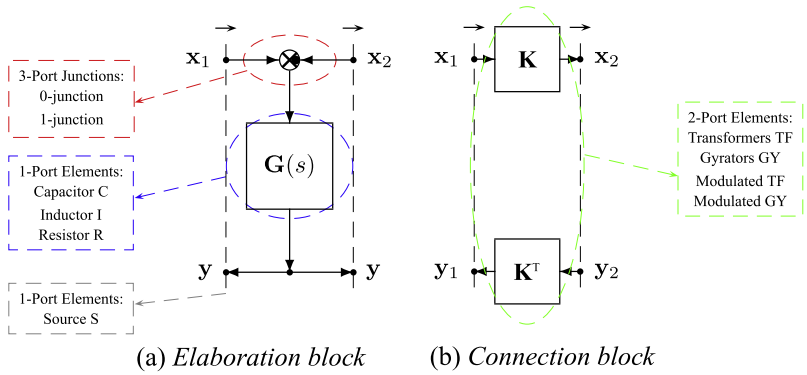

Fig. 2. POG basic blocks: *elaboration block* and *connection block* with the corresponding BG elements.

models all the 2-port elements (transformers TR and MTF, and gyrators GY and MGY) of the BG technique. In the vectorial case, matrix **K** can also be rectangular, time varying or function of other state variables.

The vertical dashed lines in Fig. 2 represent the power sections which connect the two POG basic blocks with the external world. There are no restrictions on the choice of the vectors **x** and **y** involved in each dashed line except the fact that the inner product $\langle \mathbf{x}, \mathbf{y} \rangle = \mathbf{x}^T\mathbf{y}$ must have the physical meaning of *power flowing through the section*.

2.2. Comparison BG-POG

Both BG and POG have a direct correspondence between the power ports of the system and the power ports of their graphs. Consider, for example, the POG and BG models of a DC electric motor shown in Fig. 3: the POG model is shown in the top-left and the BG model is shown in the bottom-left. The POG model can also be written using the POG vectorial form shown on the right part of Fig. 3. Note that this POG vectorial representation does not have a correspondent BG.

cThe power sections, represented by dashed lines in POG schemes, keep the two power variables coupled, thus corresponding to the power bond in BG. The POG technique uses a small arrow "→" put next to the power section to indicate (if necessary) the positive direction of power P flowing through the section. Each physical element interacts with the external world or with other physical elements by means of the power ports associated to its terminals. The two possible ways of connecting a physical element are *in series* and *in parallel*: the connection is *in series* when the two terminals of the physical element share the same through-variable; the connection is *in parallel* when the two terminals share the same across-variable. For the mechanical domain the definitions of "connection in series" and "connection in parallel" given by BG and POG are different. In BG two mechanical elements are connected in parallel (0-junction) if they share the same effort variable (Force F) while they are connected in series (1-junction) if they share the same flow variable (Velocity v). On the contrary in POG two mechanical elements are connected in parallel if they share the same across variable (Velocity v) while they are connected in series if they share the same through variable (Force F). Consider, for example, the spring and damper system shown in the left part of Fig. 4: the two physical elements are considered connected in parallel for the POG and connected in series for the BG, see also [25] for a similar example.

A comparison between the BG and POG basic blocks is shown in Figs. 5 and 6. The POG representation of a dynamic element use an elaboration block both for series and parallel connections, see Fig. 5, no matter the type of variables. The summation elements in the elaboration blocks represent the Kirchhoff's Voltage Law (KVL) when they are applied to the across variables e_1, e_2 and e (i.e. series connection) and they represent the Kirchhoff's Current Law (KCL) when applied to the through variables f_1, f_2 and f (i.e. parallel connection). Note that in BG the use of the 0-junction and 1-junction depends on the definition of the effort and flow variables.

The components representing Sources in BG are represented in POG by the power input sections, see Fig. 6. The physical elements can be connected also by means of elements that redistribute the power without storing nor dissipating energy. As reported in Fig. 6 in BG there are two types of neutral elements: the

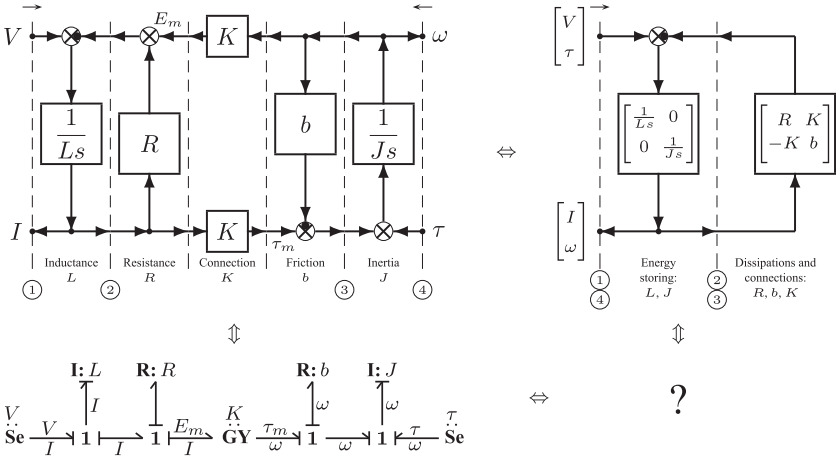

Fig. 3. POG block scheme and Bond Graph of a DC electric motor.

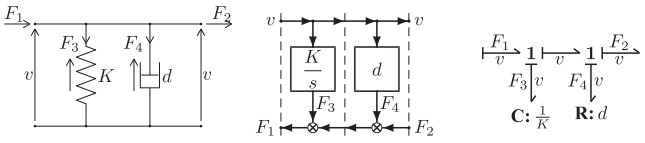

Fig. 4. A spring and damper system: POG and BG.

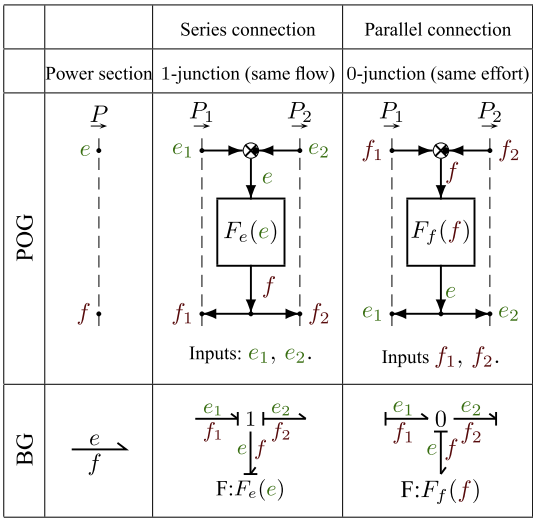

Fig. 5. Comparison of POG and BG representation of power sections and physical elements.

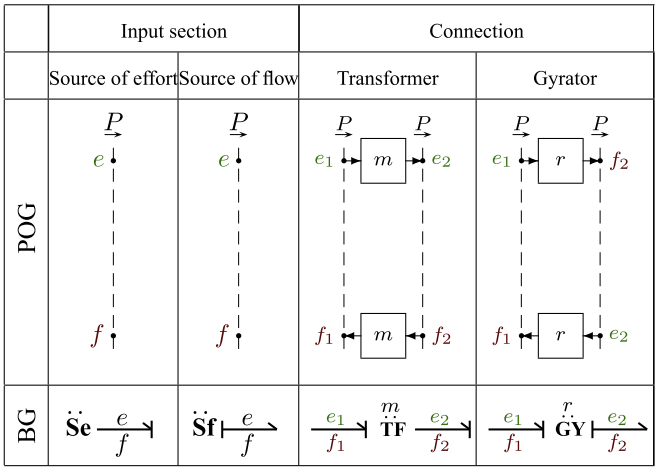

Fig. 6. Comparison of POG and BG representation of sources and connection elements.

transformers which link variables of the same type (i.e. $e_2 = me_2$ and $f_1 = mf_2$) and gyrators which link variables of different type (i.e. $f_2 = re_1$ and $f_1 = re_2$). The POG technique uses only one type of block, i.e. the connection block, for representing all types of neutral elements, no matter the type of variables. Note that the distinction between transformer and gyrators in BG is a direct consequence of the definitions chosen for the effort and flow variables.

Usually BG use a scalar notation, but also Vector Bond Graphs exist in the literature, see [27,6], with the restriction that all the vectors must be homogeneous, i.e. the vector components must be all efforts or all flows. In order to have a more compact scheme, POG often use a vectorial notation where the variable vectors can contain mixed across or through variables, see for example the POG vectorial scheme shown in the right part of Fig. 3. Like in BG, a POG can be written with derivative or integral causality, but obviously integral causality is mandatory in order to have POG models suitable for simulations.

The state space equations of a physical system can be deduced from both BG and POG. For the BG a procedure to obtain such equations is introduced in [26]. One can easily prove that using the POG approach the dynamic equations of a physical system can always be written in the following POG state-space form:

$$\begin{cases} \mathbf{L}\dot{\mathbf{x}} = -\mathbf{A}\mathbf{x} + \mathbf{B}\mathbf{u} \\ \mathbf{y} = \mathbf{B}^{\mathrm{T}}\mathbf{x} \end{cases} \tag{1}$$

where $\mathbf{x}$ is the state vector, $\mathbf{u}$ is the input vector, $\mathbf{y}$ is the output vector, $\mathbf{L}$ is the *energy matrix*, $\mathbf{A}$ is the *power matrix* and $\mathbf{B}$ is the *input matrix*. The following properties hold: the energy matrix $\mathbf{L}$ is always symmetric and positive definite $\mathbf{L} = \mathbf{L}^{\mathrm{T}} > 0$; the power matrix $\mathbf{A}$ can be decomposed in symmetric and skew-symmetric part $\mathbf{A} = \mathbf{A}_s + \mathbf{A}_w = \frac{(\mathbf{A}+\mathbf{A}^{\mathrm{T}})}{2} + \frac{(\mathbf{A}-\mathbf{A}^{\mathrm{T}})}{2}$ where $\mathbf{A}_s$ contains only dissipation terms and $\mathbf{A}_w$ only connections; for linear systems the *energy* E_s *stored in the system* can be expressed as $E_s = \frac{1}{2}\mathbf{x}^{\mathrm{T}}\mathbf{L}\mathbf{x}$; the *dissipating power* P_d *in the system* can be expressed as $P_d = \mathbf{x}^{\mathrm{T}}\mathbf{A}_s\mathbf{x}$; the skew-symmetric part $\mathbf{A}_w$ of the power matrix $\mathbf{A}$ represents the *power redistribution within the system "without losses"*, i.e. $P_d = \mathbf{x}^{\mathrm{T}}\mathbf{A}_w\mathbf{x} = 0$. The POG form (1) is similar to the notations used for the port-Hamiltonian equations in co-energy variables [12] and in generalized state-space equations [21].

2.2.1. Procedure for writing POG state-space equations from a POG scheme

The POG state-space Eq. (1) can always be obtained from the corresponding POG scheme using the following procedure (in this case the procedure has been applied to the POG model shown in Fig. 3):

1. Choose the components of the state vector $\mathbf{x}$ equal to the output power variables of the dynamic elements of the system, in the example $\mathbf{x} = [I\ \omega]^{\mathrm{T}}$.
2. Choose the components of the input vector $\mathbf{u}$ and output vector $\mathbf{y}$ equal to the power variables involved in the input and output power sections of the POG scheme, in the example $\mathbf{u} = [V\ \tau]^{\mathrm{T}}$ and $\mathbf{y} = [I\ \omega]^{\mathrm{T}}$.
3. The elements of the diagonal matrix $\mathbf{L}$ must be chosen equal to the inverse of the coefficients which characterize the dynamic elements of the system taken in the same order used for the state vector $\mathbf{x}$, in the example $\mathbf{L} = [L\,0;\ 0\,J]$.
4. The component a_{ij} of matrix $-\mathbf{A}$ is equal to the gain of the path that in the POG scheme goes from the jth state variable $\mathbf{x}_j$ to the input of the ith dynamic element, in the example $\mathbf{A} = [R\ K; -K\ b]$.
5. The component b_{ij} of matrix $\mathbf{B}$ is equal to the gain of the path that goes from the jth input variable $\mathbf{u}_j$ to the input of the ith dynamic element, $\mathbf{B} = [1\ 0; 0\ 1]$.

This procedure applied to the POG model shown in Fig. 3 provides the following state-space equations:

$$\begin{cases} \begin{bmatrix} L & 0 \\ 0 & J \end{bmatrix} \begin{bmatrix} \dot{I} \\ \dot{\omega} \end{bmatrix} = -\begin{bmatrix} R & K \\ -K & b \end{bmatrix} \begin{bmatrix} I \\ \omega \end{bmatrix} + \begin{bmatrix} 1 & 0 \\ 0 & 1 \end{bmatrix} \begin{bmatrix} V \\ \tau \end{bmatrix} \\ \begin{bmatrix} I \\ \dot{\omega} \end{bmatrix} = \begin{bmatrix} 1 & 0 \\ 0 & 1 \end{bmatrix} \begin{bmatrix} I \\ \omega \end{bmatrix} \end{cases} \tag{2}$$

As stated in [26], BG components can be combined to give a "simplified BG" with the same or approximate external behavior as the original BG. This is a kind of model reduction. As it will be discussed in Section 5, the POG technique allows to transform

and reduce the model of a dynamic system using some graphical rules thanks to which for the POG schemes the explicit expressions of the "equivalent" parameters of the reduced model can be easily obtained.

3. Description of the corker system

A picture and a photograph of the considered electromechanical corker system are shown in Fig. 7. The system is composed by two three-phase motors *ELAU ISH 070_60017*, two pulley-belt transmissions and a linear-rotary unit that contains Ball Screw grooves and Ball Spline grooves crossing each other on a single shaft (ball screw/spline). The two motors are connected to the pulley-belt transmissions and cause the linear-rotary motion of the *Tool Center Point* (TCP). In particular the upper motor actuates the screw motion and the lower motor actuates the spline motion. The motion control of the pulleys is realized by the controller *ELAU C400* included in the electric motors. A schematic representation of the structure of the considered corker system is shown in Fig. 8 together with some parameters and variables.

4. POG modeling of the system

The POG model of a physical system can always be obtained identifying the power sections of the system and following the power flows. Usually the POG schemes are drawn from left to right putting the POG block of the considered physical element between each pair of adjacent power sections.

The POG block scheme of the corker system is reported in Fig. 9. Note that in the POG scheme of Fig. 9 the power sections are denoted by numbers. The same numbers are used in Fig. 8 to denote the corresponding power sections of the physical system. In this case a POG vectorial scheme is used: each power section of the POG scheme of Fig. 9 corresponds to two power sections of the physical system shown in Fig. 8.

The power section ① is the input section of the two electrical motors and involves as power variables the voltage vector $\mathbf{V}_s$ and current vector $\mathbf{I}_s$. The blocks between power sections ① and ③ represent the dynamic model of the two electric motors, blocks between sections ③ and ④ represent the external pulleys radii, blocks between sections ④ and ⑤ represent the stiffness of the belts, blocks between sections ⑤ and ⑥ represent the internal pulleys radii, blocks between sections ⑥ and ⑦ represent the the inertias and the friction of the internal pulleys, blocks between ⑦ and ⑧ represent the interaction between the nuts of the ball screw/spline and the shaft, and blocks between sections ⑧ and ⑨ represent the dynamics of the shaft. Finally the output section ⑨ corresponds to the power section associated to the TCP of the shaft and

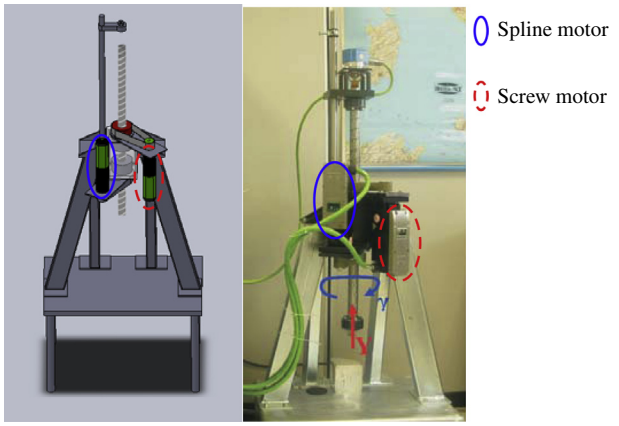

Fig. 7. Picture of the corker system and photograph of the real prototype.

involves as power variables the speed vector $\dot{\mathbf{X}}_a$ and the force vector $\mathbf{F}_{ag}$. The Vector BG model of the system corresponding to the POG of Fig. 9 is shown in Fig. 10.

4.1. POG modeling of the electrical motors

An exhaustive description of POG modeling of permanent magnet synchronous motors with an *odd* number m_s of star-connected phases can be found in [19,20]. The POG scheme of the two three-phase motors is shown in Fig. 9 between the power sections ① and ③. The meaning of the variables and parameters of the considered electric motors are reported in Table 1: subscript "e" refers to the screw motor and subscript "r" refers to the spline motor. Vectors and matrices present in the POG scheme of Fig. 9 between sections ① and ③ have the following meaning:

$$\mathbf{V}_s = \begin{bmatrix} \mathbf{V}_e \\ \mathbf{V}_r \end{bmatrix}, \quad \mathbf{I}_s = \begin{bmatrix} \mathbf{I}_e \\ \mathbf{I}_r \end{bmatrix}, \quad \boldsymbol{\omega}_m = \begin{bmatrix} \omega_e \\ \omega_r \end{bmatrix}, \quad \boldsymbol{\tau}_m = \begin{bmatrix} \tau_{me} \\ \tau_{mr} \end{bmatrix}$$

$$\mathbf{L}_s = \begin{bmatrix} \mathbf{L}_e & \mathbf{0} \\ \mathbf{0} & \mathbf{L}_r \end{bmatrix}, \quad \mathbf{R}_s = \begin{bmatrix} \mathbf{R}_e & \mathbf{0} \\ \mathbf{0} & \mathbf{R}_r \end{bmatrix}, \quad \mathbf{K}_\tau = \begin{bmatrix} \mathbf{K}_{\tau e} & \mathbf{0} \\ \mathbf{0} & \mathbf{K}_{\tau r} \end{bmatrix}$$

$$\mathbf{J}_m = \begin{bmatrix} J_e & 0 \\ 0 & J_r \end{bmatrix}, \quad \mathbf{B}_m = \begin{bmatrix} b_e & 0 \\ 0 & b_r \end{bmatrix}$$

where $\mathbf{0}$ denotes a zero matrix of proper dimension. The voltage and current stator vectors $\mathbf{V}_e$, $\mathbf{V}_r$, $\mathbf{I}_e$ and $\mathbf{I}_r$ are defined as follows:

$$\mathbf{V}_e = \begin{bmatrix} V_{e1} \\ V_{e2} \\ V_{e3} \end{bmatrix}, \quad \mathbf{V}_r = \begin{bmatrix} V_{r1} \\ V_{r2} \\ V_{r3} \end{bmatrix}, \quad \mathbf{I}_e = \begin{bmatrix} I_{e1} \\ I_{e2} \\ I_{e3} \end{bmatrix}, \quad \mathbf{I}_r = \begin{bmatrix} I_{r1} \\ I_{r2} \\ I_{r3} \end{bmatrix}$$

In the POG model of the three-phase motors, see [20], the inductances are three-dimensional dynamic elements described by the following matrices $\mathbf{L}_e$ and $\mathbf{L}_r$:

$$\mathbf{L}_e = \begin{bmatrix} L_{e0} & M_{e0}\cos\frac{2\pi}{3} & M_{e0}\cos\frac{4\pi}{3} \\ M_{e0}\cos\frac{2\pi}{3} & L_{e0} & M_{e0}\cos\frac{2\pi}{3} \\ M_{e0}\cos\frac{4\pi}{3} & M_{e0}\cos\frac{2\pi}{3} & L_{e0} \end{bmatrix}$$

$$\mathbf{L}_r = \begin{bmatrix} L_{r0} & M_{r0}\cos\frac{2\pi}{3} & M_{r0}\cos\frac{4\pi}{3} \\ M_{r0}\cos\frac{2\pi}{3} & L_{r0} & M_{r0}\cos\frac{2\pi}{3} \\ M_{r0}\cos\frac{4\pi}{3} & M_{r0}\cos\frac{2\pi}{3} & L_{r0} \end{bmatrix}$$

where $L_{e0} = L_e - M_{e0}$ and $L_{r0} = L_r - M_{r0}$. The structure of matrices $\mathbf{L}_e$ and $\mathbf{L}_r$ comes directly from the differential equations describing the electrical part of the motors. The resistance matrices $\mathbf{R}_e$ and $\mathbf{R}_r$ are diagonal: $\mathbf{R}_e = R_e\mathbf{I}_3$ and $\mathbf{R}_r = R_r\mathbf{I}_3$ where $\mathbf{I}_3$ is the 3×3 identity matrix. The torque vectors $\mathbf{K}_{\tau e}$ and $\mathbf{K}_{\tau r}$ are defined in [20]. They satisfy relations $\mathbf{K}_\tau^{\mathrm{T}}\mathbf{I}_s = \boldsymbol{\tau}_e$ and $\mathbf{K}_\tau\boldsymbol{\omega}_m = \mathbf{E}_m$ where $\boldsymbol{\tau}_e$ is the motor torque vector and $\mathbf{E}_m$ is the back-electromotive force vector.

4.2. POG modeling of the belt transmission system and the linear-rotary unit

The POG scheme of the belt transmission system is shown in Fig. 9 between the power sections ③ and ⑦. The meaning of the variables and parameters of the transmission and linear-rotary unit are reported in Table 2. The vectors and matrices present in the block scheme have the following meaning:

$$\mathbf{F}_c = \begin{bmatrix} F_e \\ F_r \end{bmatrix}, \quad \boldsymbol{\omega}_t = \begin{bmatrix} \omega_{te} \\ \omega_{tr} \end{bmatrix}, \quad \boldsymbol{\tau}_t = \begin{bmatrix} \tau_{te} \\ \tau_{tr} \end{bmatrix}$$

$$\mathbf{R}_1 = \begin{bmatrix} R_{1e} & 0 \\ 0 & R_{1r} \end{bmatrix}, \quad \mathbf{K}_c = \begin{bmatrix} K_{ce} & 0 \\ 0 & K_{cr} \end{bmatrix}, \quad \mathbf{R}_2 = \begin{bmatrix} R_{2e} & 0 \\ 0 & R_{2r} \end{bmatrix}$$

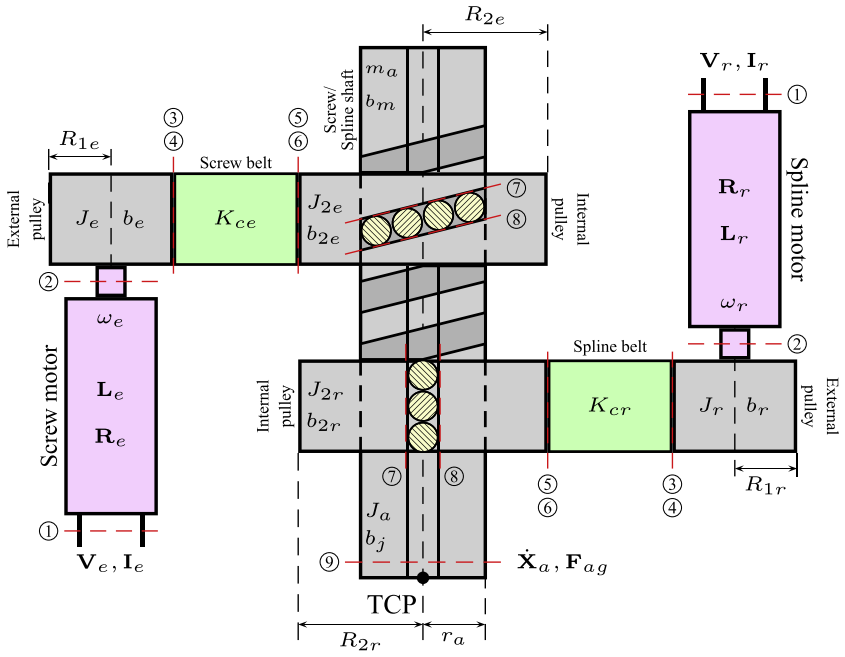

Fig. 8. Structure and parameters of the considered corker system: electric motors, pulleys, belts and screw/spline shaft.

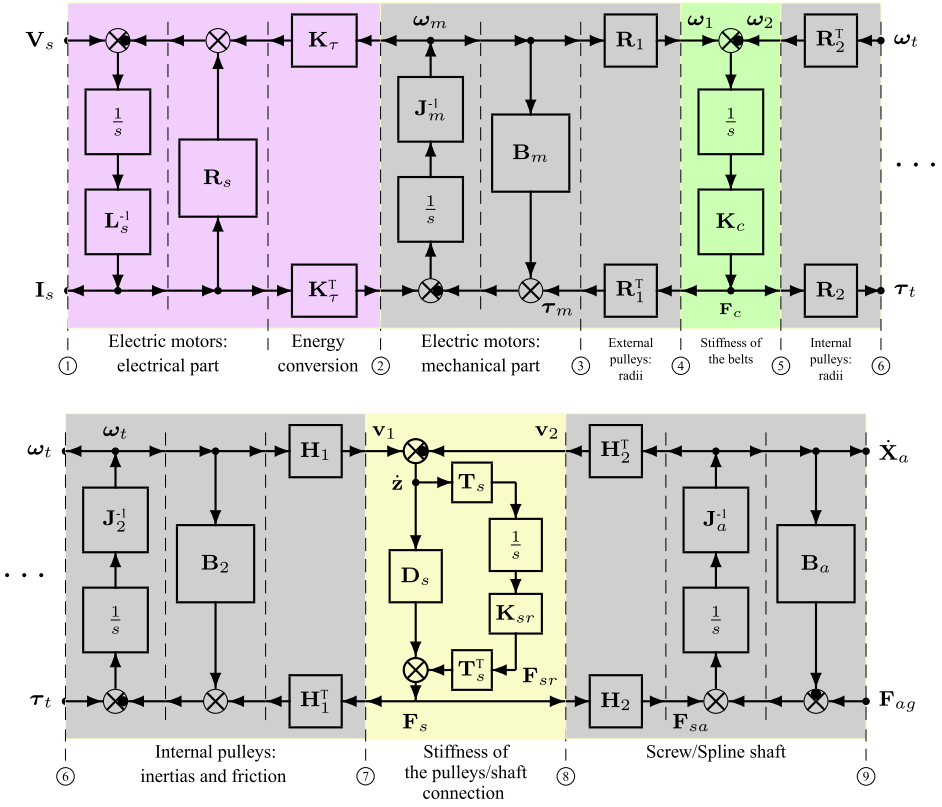

Fig. 9. POG scheme of the corking system composed by the three-phase electric motors, the pulley-belt transmissions, the nuts of the ball screw and the ball spline and the shaft.

$$\mathbf{J}_2 = \begin{bmatrix} J_{2e} & 0 \\ 0 & J_{2r} \end{bmatrix}, \quad \mathbf{B}_2 = \begin{bmatrix} b_{2e} & 0 \\ 0 & b_{2r} \end{bmatrix}, \quad \mathbf{H}_1 = \begin{bmatrix} r_a \cos\alpha & 0 \\ r_a \sin\alpha & 0 \\ 0 & r_a \\ 0 & 0 \end{bmatrix}$$

Matrix $\mathbf{H}_1$ satisfies the following relation:

$$\mathbf{H}_1 \boldsymbol{\omega}_t = \begin{bmatrix} r_a \omega_{te} \cos\alpha \\ r_a \omega_{te} \sin\alpha \\ r_a \omega_{tr} \\ 0 \end{bmatrix} = \begin{bmatrix} v_{ek1} \\ v_{ed1} \\ v_{rk1} \\ 0 \end{bmatrix} = \mathbf{v}_1$$

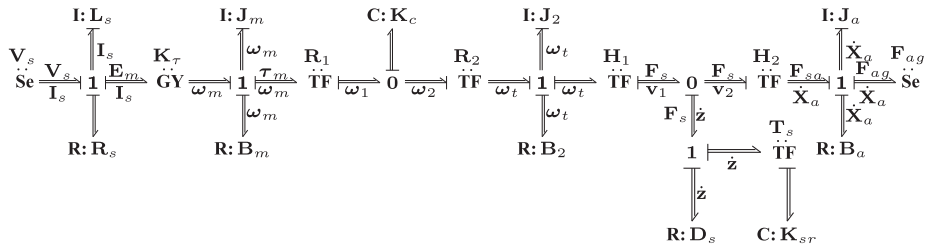

Fig. 10. Vector Bond Graph of the corking system.

Table 1
Meaning of variables and parameters of the electric motors.

V_{ei}, I_{ei}	Voltage and current of the ith phase of the screw motor
V_{ri}, I_{ri}	Voltage and current of the ith phase of the spline motor
R_e, R_r	Stator phase resistance of screw and spline motors
L_e	Stator self induction coefficient of screw motor
M_{e0}	Maximum value of the stator mutual inductance of screw motor
L_r	Stator self induction coefficient of spline motor
M_{r0}	Maximum value of the stator mutual inductance of spline motor
J_e, b_e	Moment of inertia and friction coefficient of screw motor
J_r, b_r	Moment of inertia and friction coefficient of spline motor
ω_e, ω_r	Angular velocity of screw and spline motors

Table 2
Meaning of variables and parameters of the belt transmission system and linear-rotary unit.

F_e, F_r	Tangential forces of the screw and spline belts
ω_{te}, ω_{tr}	Angular velocity of screw and spline pulleys
τ_{te}, τ_{tr}	Torques acting on internal pulleys
x, θ	Translational and rotational shaft positions
$\dot{x}$, $\dot{\theta}$	Translational and rotational shaft velocities
R_{1e}, R_{1r}	Radii of external screw and spline pulleys
K_{ce}, K_{cr}	Stiffness of screw and spline belts
R_{2e}, R_{2r}	Radii of internal screw and spline pulleys
J_{2e}, b_{2e}	Inertia and friction coefficient of the internal screw pulley
J_{2r}, b_{2r}	Inertia and friction coefficient of the internal spline pulley
r_a, l_a	Radius and length of the shaft
α	Angle between the screw groove and the shaft axle
K_{se}, d_{se}	Stiffness and friction coefficient between screw pulley and screw groove
K_{sr}, d_{sr}	Stiffness and friction coefficient between spline pulley and spline groove
m_a, b_m	Mass and linear friction coefficient of the shaft
J_a, b_j	Inertia and rotational friction coefficient of the shaft

where v_{ek1}, v_{ed1} and v_{rk1} are the projections of the pulleys velocities ω_{te} and ω_{tr} along the tangential reference frames Σ_e and Σ_r of the screw groove and vertical spline groove, respectively, as it is shown in Fig. 11.

The POG scheme of the linear-rotary unit is shown in Fig. 9 between power sections ⑦ and ⑨. The elastic/dissipative interaction between the internal pulleys and the shaft is modeled in Fig. 9 by the blocks present between sections ⑦ and ⑧ and it is characterized by the following matrices:

$$\mathbf{D}_s = \begin{bmatrix} 0 & 0 & 0 & 0 \\ 0 & d_{se} & 0 & 0 \\ 0 & 0 & 0 & 0 \\ 0 & 0 & 0 & d_{sr} \end{bmatrix}, \quad \mathbf{K}_{sr} = \begin{bmatrix} K_{se} & 0 \\ 0 & K_{sr} \end{bmatrix}, \quad \mathbf{T}_s = \begin{bmatrix} 1 & 0 & 0 & 0 \\ 0 & 0 & 1 & 0 \end{bmatrix}$$

where $\mathbf{D}_s$ is the friction matrix, $\mathbf{K}_{sr}$ is the stiffness matrix and $\mathbf{T}_s$ is a proper selection matrix. Friction matrix $\mathbf{D}_s$ has only two non-zero elements because friction has been inserted only along the directions of the vertical and screw grooves, while the stiffnesses K_{se} and K_{sr} has been inserted only along the directions normal to the grooves, see Fig. 11. The inertial dynamics of the shaft is described in Fig. 9 by the POG blocks present between sections ⑧ and ⑨ and it is characterized by the following vectors and matrices:

$$\mathbf{H}_2^{\mathrm{T}} = \begin{bmatrix} -\sin\alpha & r_a\cos\alpha \\ \cos\alpha & r_a\sin\alpha \\ 0 & r_a \\ 1 & 0 \end{bmatrix}, \quad \mathbf{J}_a = \begin{bmatrix} m_a & 0 \\ 0 & J_a \end{bmatrix}, \quad \mathbf{B}_a = \begin{bmatrix} b_m & 0 \\ 0 & b_j \end{bmatrix}$$

$$\dot{\mathbf{X}}_a = \begin{bmatrix} \dot{x} \\ \dot{\theta} \end{bmatrix}, \quad \mathbf{F}_g = \begin{bmatrix} -m_a g \\ 0 \end{bmatrix}, \quad \mathbf{F}_{ag} = \mathbf{F}_a + \mathbf{F}_g$$

The input vector $\mathbf{F}_{ag}$ represents the sum of the external forces $\mathbf{F}_a$ and the weight forces $\mathbf{F}_g$ acting on the shaft. Matrix $\mathbf{H}_2$, similarly to matrix $\mathbf{H}_1$, satisfies the following relation:

$$\mathbf{H}_2^{\mathrm{T}}\dot{\mathbf{X}}_a = \begin{bmatrix} -\dot{x}\sin\alpha + r_a\dot{\theta}\cos\alpha \\ \dot{x}\cos\alpha + r_a\dot{\theta}\sin\alpha \\ r_a\dot{\theta} \\ \dot{x} \end{bmatrix} = \begin{bmatrix} v_{ek2} \\ v_{ed2} \\ v_{rk2} \\ v_{rd2} \end{bmatrix} = \mathbf{v}_2$$

where v_{ek2}, v_{ed2}, v_{rk2} and v_{rd2} are the projections of the translational velocity $\dot{x}$ and rotational velocity $\dot{\theta}$ of the shaft along the tangential reference frames Σ_e and Σ_r of the grooves.

4.3. POG state space dynamic equations

The dynamic equations of the POG scheme shown in Fig. 9 between sections ⑥ and ⑨ can be written in the POG state-space form (1) if matrices $\mathbf{L}$, $\mathbf{A}$, $\mathbf{B}$ and vectors $\mathbf{x}$, $\mathbf{u}$ and $\mathbf{y}$ are defined as follows:

$$\mathbf{L} = \begin{bmatrix} \mathbf{J}_2 & \mathbf{0} & \mathbf{0} \\ \mathbf{0} & \mathbf{K}_{sr}^{-1} & \mathbf{0} \\ \mathbf{0} & \mathbf{0} & \mathbf{J}_a \end{bmatrix}, \quad \mathbf{B} = \begin{bmatrix} \mathbf{I}_2 & \mathbf{0} \\ \mathbf{0} & \mathbf{0} \\ \mathbf{0} & \mathbf{I}_2 \end{bmatrix}, \quad \mathbf{x} = \begin{bmatrix} \boldsymbol{\omega}_t \\ \mathbf{F}_{sr} \\ \dot{\mathbf{X}}_a \end{bmatrix}, \quad \mathbf{u} = \begin{bmatrix} \boldsymbol{\tau}_t \\ \mathbf{F}_{ag} \end{bmatrix} \tag{3}$$

$$\mathbf{A} = \begin{bmatrix} \mathbf{B}_2 + \mathbf{H}_1^{\mathrm{T}}\mathbf{D}_s\mathbf{H}_1 & \mathbf{H}_1^{\mathrm{T}}\mathbf{T}_s^{\mathrm{T}} & -\mathbf{H}_1^{\mathrm{T}}\mathbf{D}_s\mathbf{H}_2^{\mathrm{T}} \\ -\mathbf{T}_s\mathbf{H}_1 & \mathbf{0} & \mathbf{T}_s\mathbf{H}_2^{\mathrm{T}} \\ -\mathbf{H}_2\mathbf{D}_s\mathbf{H}_1 & -\mathbf{H}_2\mathbf{T}_s^{\mathrm{T}} & \mathbf{B}_a + \mathbf{H}_2\mathbf{D}_s\mathbf{H}_2^{\mathrm{T}} \end{bmatrix}, \quad \mathbf{y} = \begin{bmatrix} \boldsymbol{\omega}_t \\ \dot{\mathbf{X}}_a \end{bmatrix} \tag{4}$$

where $\mathbf{I}_2$ is the 2×2 identity matrix. These matrices and vectors have been obtained using the step-by-step procedure described in Section 2.2 which allows to convert a POG scheme in the corresponding state space form.

5. POG model reduction

It can be easily proved that when an eigenvalue of matrix $\mathbf{L}$ tends to zero (or to infinity), the POG system (1) degenerates towards a lower dimension system which maintains the same POG structure given in (1).

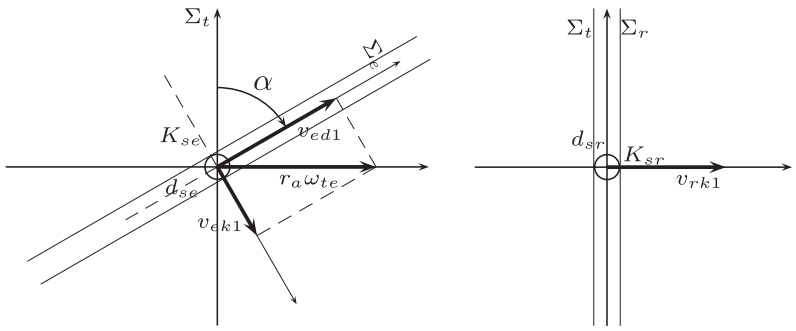

Fig. 11. Decomposition of tangential velocities of the pulleys $r_a\omega_{te}$ and $r_a\omega_{tr}$ along the screw groove and the vertical spline groove.

5.1. Reduced model when $\mathbf{K}_{sr} \to \infty$

To show how to obtain a reduced POG system consider, for example, the POG system (1), (3) and (4) when $\mathbf{K}_{sr} \to \infty$, that is when the stiffness coefficients K_{se} and K_{sr} between the nuts and the shaft tend to infinity. When $\mathbf{K}_{sr} \to \infty$ in system (1) the following internal constraint appears:

$$\mathbf{T}_s\mathbf{H}_1\boldsymbol{\omega}_t - \mathbf{T}_s\mathbf{H}_2^{\mathrm{T}}\dot{\mathbf{X}}_a = \mathbf{0}$$

which leads to the following relation:

$$\dot{\mathbf{X}}_a = (\mathbf{T}_s\mathbf{H}_2^{\mathrm{T}})^{-1}\mathbf{T}_s\mathbf{H}_1\,\boldsymbol{\omega}_t \tag{5}$$

Using (5), the following "rectangular" and constant state space transformation $\mathbf{x} = \mathbf{T}_0\mathbf{z}$ can be written:

$$\mathbf{x} = \mathbf{T}_0\mathbf{z} \quad \leftrightarrow \quad \underbrace{\begin{bmatrix}\boldsymbol{\omega}_t\\ \mathbf{F}_{sr}\\ \dot{\mathbf{X}}_a\end{bmatrix}}_{\mathbf{x}} = \underbrace{\begin{bmatrix}\mathbf{I}_2\\ \mathbf{0}\\ (\mathbf{T}_s\mathbf{H}_2^{\mathrm{T}})^{-1}\mathbf{T}_s\mathbf{H}_1\end{bmatrix}}_{\mathbf{T}_0}\underbrace{\boldsymbol{\omega}_t}_{\mathbf{z}} \tag{6}$$

This transformation relates the old state vector $\mathbf{x}$ to the new state vector $\mathbf{z} = \boldsymbol{\omega}_t$. Note that transformation (6) is not invertible because matrix $\mathbf{T}_0$ is rectangular. Applying the "congruent transformation" (6) to the system (1), one obtains the following transformed and reduced POG system:

$$\begin{cases}\overline{\mathbf{L}}\dot{\mathbf{z}} &= -\overline{\mathbf{A}}\mathbf{z} + \overline{\mathbf{B}}\mathbf{u}\\ \mathbf{y} &= \overline{\mathbf{B}}^{\mathrm{T}}\mathbf{z}\end{cases} \tag{7}$$

where matrices $\overline{\mathbf{L}}$, $\overline{\mathbf{A}}$ and $\overline{\mathbf{B}}$ are defined as follows:

$$\overline{\mathbf{L}} = \mathbf{T}_0^{\mathrm{T}}\mathbf{L}\mathbf{T}_0, \quad \overline{\mathbf{A}} = \mathbf{T}_0^{\mathrm{T}}\mathbf{A}\mathbf{T}_0, \quad \overline{\mathbf{B}} = \mathbf{T}_0^{\mathrm{T}}\mathbf{B}. \tag{8}$$

For the considered example the transformed matrices $\overline{\mathbf{L}}$, $\overline{\mathbf{A}}$ and $\overline{\mathbf{B}}$ have the following structure:

$$\overline{\mathbf{L}} = \begin{bmatrix} J_{2e} + m_a r_a^2\cot^2(\alpha) & -m_a r_a^2\cot^2(\alpha)\\ -m_a r_a^2\cot^2(\alpha) & J_{2r} + J_a + m_a r_a^2\cot^2(\alpha)\end{bmatrix} = \mathbf{J}_t \tag{9}$$

$$\overline{\mathbf{A}} = \begin{bmatrix}A_{11} & A_{12}\\ A_{12} & A_{22}\end{bmatrix} = \mathbf{A}_t, \quad \overline{\mathbf{B}} = \begin{bmatrix}\mathbf{I}_2 & \mathbf{T}_a^{\mathrm{T}}\end{bmatrix} \tag{10}$$

where parameters A_{11}, A_{12} and A_{22} are

$$A_{11} = b_{2e} - (b_m + d_{sr})r_a^2 + (b_m + d_{se} + d_{sr})r_a^2\csc^2(\alpha)$$

$$A_{12} = -\frac{1}{2}r_a^2(b_m + 2d_{se} + d_{sr} + (b_m + d_{sr})\cos(2\alpha))\csc^2(\alpha)$$

$$A_{22} = b_{2r} + b_j - (b_m + d_{sr})r_a^2 + (b_m + d_{se} + d_{sr})r_a^2\csc^2(\alpha)$$

and matrix $\mathbf{T}_a$ is

$$\mathbf{T}_a = \begin{bmatrix}-r_a\cot(\alpha) & r_a\cot(\alpha)\\ 0 & 1\end{bmatrix}$$

A POG graphical representation of the reduced system 7, 9 and 10 is shown in Fig. 12 between the power sections ⑥ and ⑨. In the same figure the POG scheme between the power sections ③ and ⑥ represents the stiffness of the belts and the radii of the external and internal pulleys.

Remark 2. The POG "congruent transformations" (7)-(8) are characterized by the following properties: (a) when matrix $\mathbf{T}_0$ is rectangular the system is transformed and reduced at the same time; (b) they do not require the inversion of the transformation matrix $\mathbf{T}_0$ as it happens for the "similarity" transformations; (c) the transformed system (7) keeps the same POG properties of the original system (1): stability, dissipativity, input–output power sections, physical insight, etc.

Other reduction methods based on the use of a rectangular matrix $\mathbf{T}$ can be found in literature, see for example [12], but these methods require the columns of matrix $\mathbf{T}$ to be orthonormal. More details and examples about POG congruent transformations can be found in [14,22].

5.2. Procedure for writing the full and reduced POG models

Obtaining the dynamic equations of a complex physical system when some of the internal parameters are equal to zero or to infinity is often NOT an easy task. The POG approach provides the following simple methodology to face this task:

1. Analyze the physical system putting in evidence the input–output power sections and the power flows within the system. See for example Fig. 8.
2. Write down the POG block scheme of the considered physical system starting from the inputs and introducing fictitious additional elements whenever it is useful to simplify the writing down of the dynamic model which must be characterized only by integral causality. In the example of Fig. 9 the fictitious element "Stiffness of the pulleys/shaft connection" between sections ⑦ and ⑧ has been inserted to simplify the system modeling.
3. Obtain the state space equations of the system in the POG form (1) using the procedure described in Section 2.2. See Eqs. (1), (3) and (4).
4. Obtain the static relations between the state variables when in system (1) the additional fictitious parameters tend to zero or to infinity. See the static relation (5).
5. Build a rectangular state-space congruent transformation $\mathbf{x} = \mathbf{T}_0\mathbf{z}$ using the static relations obtained above. See the congruent transformation (6).
6. Apply the congruent transformation $\mathbf{x} = \mathbf{T}_0\mathbf{z}$ to system (1) and obtain the transformed and reduced system in the POG form (7) and (8). See the reduced system (7), (9) and (10).

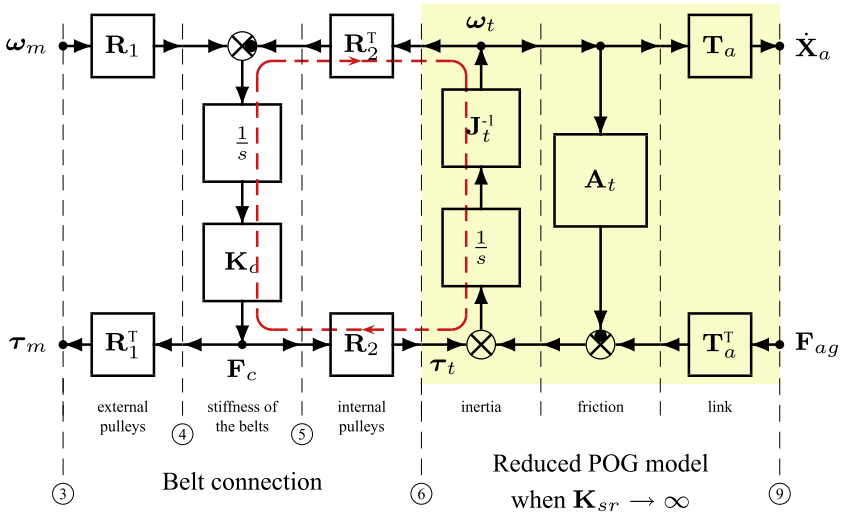

Fig. 12. Reduced POG scheme of the system pulleys & screw/spline shaft with belt connection and inversion of a path.

This methodology is similar to the Singular Perturbation approach, see [23], when the dynamics of the additional fictitious elements is much faster than the dynamics of the physical elements present in the reduced order system.

5.3. Input–output static model when $\mathbf{K}_c \to \infty$ and $\mathbf{J}_t \to 0$

The state-space equations $\tilde{\mathbf{L}}\dot{\tilde{\mathbf{x}}} = -\tilde{\mathbf{A}}\tilde{\mathbf{x}} + \tilde{\mathbf{B}}\tilde{\mathbf{u}}$ and $\tilde{\mathbf{y}} = \tilde{\mathbf{B}}^{\mathrm{T}}\tilde{\mathbf{x}}$ of the POG scheme shown in Fig. 12 can be written as follows:

$$\begin{cases} \underbrace{\begin{bmatrix} \mathbf{K}_c^{-1} & \mathbf{0} \\ \mathbf{0} & \mathbf{J}_t \end{bmatrix}}_{\tilde{\mathbf{L}}} \underbrace{\begin{bmatrix} \dot{\mathbf{F}}_c \\ \dot{\boldsymbol{\omega}}_t \end{bmatrix}}_{\dot{\tilde{\mathbf{x}}}} = -\underbrace{\begin{bmatrix} \mathbf{0} & \mathbf{R}_2^{\mathrm{T}} \\ -\mathbf{R}_2 & \mathbf{A}_t \end{bmatrix}}_{\tilde{\mathbf{A}}} \underbrace{\begin{bmatrix} \mathbf{F}_c \\ \boldsymbol{\omega}_t \end{bmatrix}}_{\tilde{\mathbf{x}}} + \underbrace{\begin{bmatrix} \mathbf{R}_1 & \mathbf{0} \\ \mathbf{0} & \mathbf{T}_a^{\mathrm{T}} \end{bmatrix}}_{\tilde{\mathbf{B}}} \underbrace{\begin{bmatrix} \boldsymbol{\omega}_m \\ \mathbf{F}_{ag} \end{bmatrix}}_{\tilde{\mathbf{u}}} \\ \underbrace{\begin{bmatrix} \boldsymbol{\tau}_m \\ \dot{\mathbf{X}}_a \end{bmatrix}}_{\tilde{\mathbf{y}}} = \underbrace{\begin{bmatrix} \mathbf{R}_1^{\mathrm{T}} & \mathbf{0} \\ \mathbf{0} & \mathbf{T}_a \end{bmatrix}}_{\tilde{\mathbf{B}}^{\mathrm{T}}} \underbrace{\begin{bmatrix} \mathbf{F}_c \\ \boldsymbol{\omega}_t \end{bmatrix}}_{\tilde{\mathbf{x}}} \end{cases} \tag{11}$$

When $\mathbf{K}_c \to \infty$ and $\mathbf{J}_t \to 0$ the input–output static model of the considered system can be obtained in two different and equivalent ways: analytically and graphically.

5.3.1. Analytical solution

When the stiffness matrix $\mathbf{K}_c$ of the belts tends to infinity and the inertia matrix $\mathbf{J}_t$ of the pulleys/shaft tend to zero, the energy matrix $\tilde{\mathbf{L}}$ tends to zero and the dynamic system (11) becomes static with the following structure:

$$\begin{cases} \mathbf{0} = -\tilde{\mathbf{A}}\tilde{\mathbf{x}} + \tilde{\mathbf{B}}\tilde{\mathbf{u}} \\ \tilde{\mathbf{y}} = \tilde{\mathbf{B}}^{\mathrm{T}}\tilde{\mathbf{x}} \end{cases} \tag{12}$$

If matrix $\tilde{\mathbf{A}}$ is invertible, from (12) one obtains the following input–output static relation:

$$\tilde{\mathbf{y}} = \tilde{\mathbf{B}}^{\mathrm{T}}\tilde{\mathbf{A}}^{-1}\tilde{\mathbf{B}}\tilde{\mathbf{u}} \quad \Longleftrightarrow \quad \underbrace{\begin{bmatrix} \boldsymbol{\tau}_m \\ \dot{\mathbf{X}}_a \end{bmatrix}}_{\tilde{\mathbf{y}}} = \underbrace{\begin{bmatrix} \mathbf{A}_p & -\mathbf{T}_p^{\mathrm{T}} \\ \mathbf{T}_p & \mathbf{0} \end{bmatrix}}_{\tilde{\mathbf{B}}^{\mathrm{T}}\tilde{\mathbf{A}}^{-1}\tilde{\mathbf{B}}} \underbrace{\begin{bmatrix} \boldsymbol{\omega}_m \\ \mathbf{F}_{ag} \end{bmatrix}}_{\tilde{\mathbf{u}}} \tag{13}$$

where $\mathbf{A}_p = \mathbf{R}_1^{\mathrm{T}}\mathbf{R}_2^{-1}\mathbf{A}_t\mathbf{R}_2^{-\mathrm{T}}\mathbf{R}_1$ and matrix $\mathbf{T}_p$ has the following form:

$$\mathbf{T}_p = \mathbf{T}_a\mathbf{R}_2^{-\mathrm{T}}\mathbf{R}_1 = \begin{bmatrix} r_a \cot(\alpha)\frac{R_{1e}}{R_{2e}} & -r_a \cot(\alpha)\frac{R_{1r}}{R_{2r}} \\ 0 & -\frac{R_{1r}}{R_{2r}} \end{bmatrix}$$

A POG graphical representation of the static model (13) is shown on the right of Fig. 13.

5.3.2. Graphical solution

The input–output static model (13) can also be obtained "graphically" acting directly on the POG scheme of Fig. 12: inverting the path corresponding to the red dashed line one obtains the equivalent POG scheme shown on the left of Fig. 13. Note that inverting this path the dynamic elements change their causality from integral to derivative. When $\mathbf{K}_c \to \infty$ and $\mathbf{J}_t \to 0$, the corresponding dynamic elements $\mathbf{K}_c^{-1}$ and $\mathbf{J}_t$ in Fig. 13 can be eliminated obtaining the POG input–output static model shown on the right of Fig. 13. One can easily verify that the following static equations:

$$\begin{aligned} \boldsymbol{\tau}_m &= \mathbf{A}_p\,\boldsymbol{\omega}_m - \mathbf{T}_p^{\mathrm{T}}\mathbf{F}_{ag} \\ \dot{\mathbf{X}}_a &= \mathbf{T}_p\,\boldsymbol{\omega}_m \end{aligned} \tag{14}$$

obtained graphically from the POG static model of Fig. 13, are completely equivalent to the static equations obtained in (13) using the analytical approach.

6. Simulation

The POG model of the corking machine obtained in the previous sections has been implemented in Simulink using the block scheme shown in Fig. 14. Note that the Simulink block scheme between sections ① and ⑥ is an exact copy of the POG scheme shown in the upper part of Fig. 9, and the Simulink blocks between sections ⑥ and ⑨ are equal to the corresponding POG reduced model shown in Fig. 12 between sections ⑥ and ⑨.

The system parameters have been identified using experimental data obtained using the prototype shown on the right of Fig. 7. The time behaviors of the vertical position x and the angular position θ of the shaft used in the experimental test are shown in Fig. 15. The measured angular speeds of the two electrical motors have been used in simulation as the reference signals of two PID speed controllers for the electrical motors, see the Simulink block "CONTROL" in Fig. 14. The trajectory of the TCP at the end of the shaft has been planned as follows, see Fig. 15: ⓐ the TCP descends to grasp the cap, ⓑ the TCP rises, ⓒ the TCP descends and approaches the bottle neck, ⓓ the TCP screws the cap on the bottle and ⓔ the TCP moves back to initial position. During the first 8 s the shaft moves only vertically (note that the angular position is

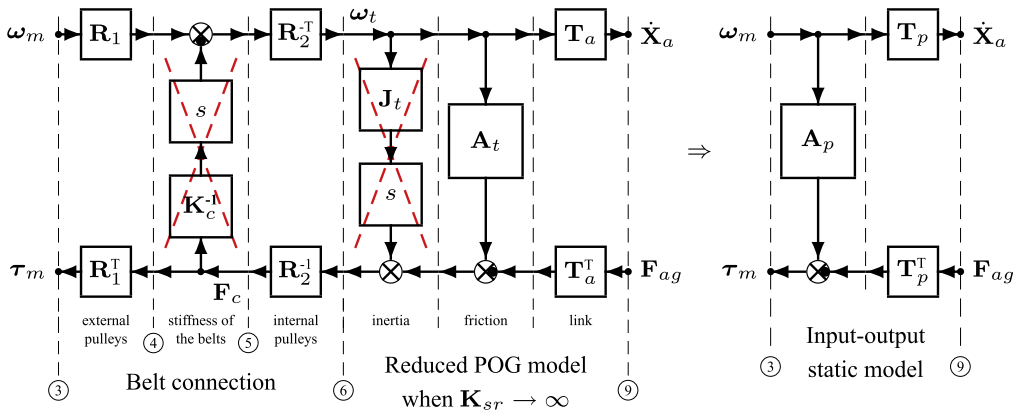

Fig. 13. Transformed POG scheme. When $\mathbf{K}_c \to \infty$ and $\mathbf{J}_t \to 0$ the system becomes rigid.

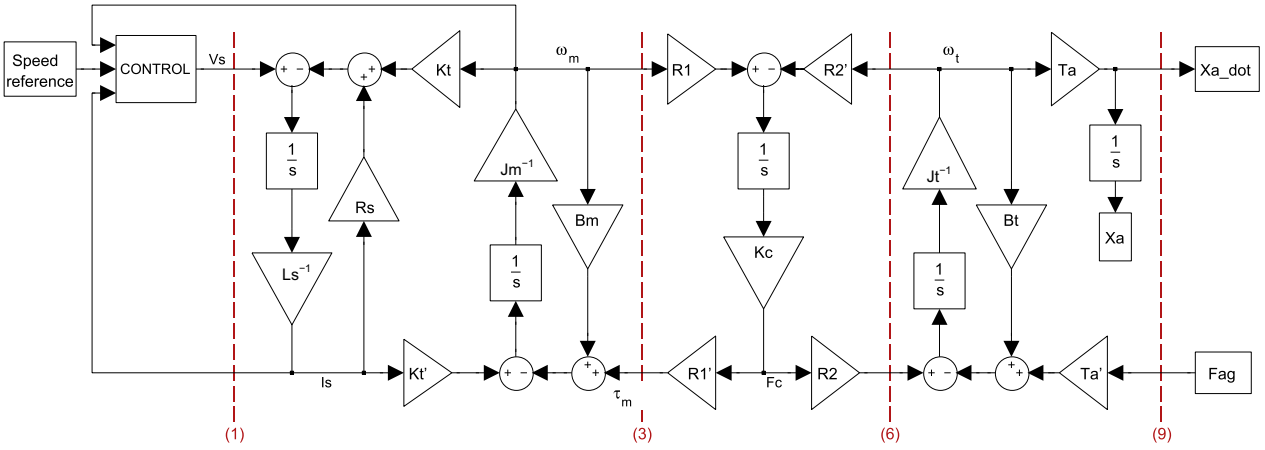

Fig. 14. Simulink block scheme of the corking machine.

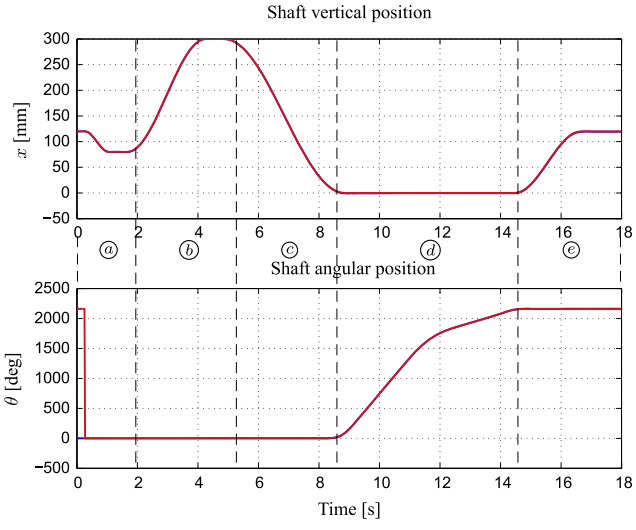

Fig. 15. Vertical and angular position of the shaft: simulated (blue) and measured (red). (For interpretation of the references to colour in this figure legend, the reader is referred to the web version of this article.)

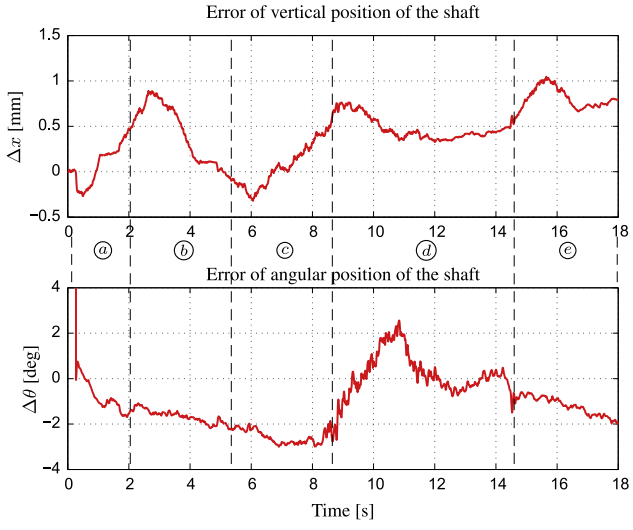

Fig. 16. Errors of vertical position and angular position of the shaft.

constant during this time). Then the vertical position remains constant while the shaft rotates (this corresponds to the screwing of the cap). Finally, after 14 s, the rotary motion stops and the shaft is moved back to the initial position.

In Fig. 15 the measured positions of the shaft are shown and compared with the positions obtained in simulation using the Simulink block scheme of Fig. 14: the time-behaviors are quite similar and practically overlying. The difference between the simulated

and measured positions are shown in Fig. 16: the maximum error of vertical position x is about 1 mm, while the maximum error of angular position θ is about 3 deg. These results clearly prove that the POG reduced model obtained in the previous sections describes very well the dynamics of the considered corking system.

7. Conclusion

In this paper the Power-Oriented-Graphs energy-based graphical technique has been used for modeling an automatic corking machine for threaded plastic caps. A comparison of POG against Bond Graphs has been given to show differences and common aspects of the two modeling techniques. Taking advantages from the POG capability for modeling, transforming and reducing dynamic systems, both an extended and reduced model for the considered automatic corking machine have been given. The simulation results, compared with experimental data obtained using a prototype of the machine, show a good match thus confirming the effectiveness of the proposed model.

References

[1] Paynter HM. Analysis and design of engineering systems. Camb., MA: MIT-Press; 1961.
[2] Karnopp DC, Margolis DL, Rosemberg RC. System dynamics – modeling and simulation of mechatronic systems. 3rd ed. WileyInterscience; 2000.
[3] Zanasi R. The power-oriented graphs technique: system modeling and basic properties. In: Proc. of 2010 IEEE vehicle power and propulsion conference (VPPC); 2010. p. 1–6.
[4] Firestone FA. A new analogy between mechanical and electrical systems. J Acoust Soc, Michigan 1933.
[5] Mercieca JC, Verhille JN, Bouscayrol A. Energetic macroscopic representation of a subway traction system for a simulation model. In: Proceeding of IEEE-ISIE 2004; May 2004. p. 1519–24.
[6] Zanasi R, Geitner GH, Bouscayrol A, Lhomme W. Different energetic techniques for modelling traction drives. ELECTRIMACS 2008, Qubec, Canada, June 8–11; 2008.
[7] Zanasi R, Grossi F. Differences and common aspects of POG and EMR energy-based graphical techniques. In: Proc. of IEEE vehicle power and propulsion conference VPPC; 2011. p. 1, 6.
[8] Chhabra R, Emami MR. Holistic system modeling in mechatronics. Mechatronics 2011;21(1):166–75. ISSN: 0957-4158.
[9] Vijay P, Samantaray AK, Mukherjee A. A bond graph model-based evaluation of a control scheme to improve the dynamic performance of a solid oxide fuel cell. Mechatronics 2009;19(4):489–502. ISSN: 0957-4158.
[10] Touati Y, Merzouki R, Bouamama BO. Robust diagnosis to measurement uncertainties using bond graph approach: application to intelligent autonomous vehicle. Mechatronics 2012;22(8):1148–60. ISSN: 0957-4158.
[11] Reis T, Stykel T. PABTEC: passivity-preserving balanced truncation for electrical circuits. IEEE Trans Comput-Aid Des Integr Circ Syst 2010;29(9):1354–67.
[12] Polyuga RV, van der Schaft A. Structure preserving model reduction of port-Hamiltonian systems by moment matching at infinity. Automatica 2010;46(4):665–72. ISSN: 0005-1098.
[13] Antoulas AC. A new result on passivity preserving model reduction. Syst Contr Lett 2005;54(4):361–74. ISSN: 0167-6911.
[14] Zanasi R, Grossi F. The POG technique for modeling planetary gears and hybrid automotive systems. In: Proc. of IEEE vehicle power and propulsion conference, VPPC; 2009. p. 1301–7.
[15] Sollmann KS, Jouaneh MK, Lavender D. Dynamic modeling of a two-axis, parallel, H-frame-type XY positioning system, mechatronics. IEEE/ASME Trans 2010;15(2):280–90.
[16] Kim Min-Seok, Chung Sung-Chong. Integrated design methodology of ball-screw driven servomechanisms with discrete controllers. Part I: Modelling and performance analysis. Mechatronics 2006;16(8):491–502. ISSN: 0957-4158.
[17] Kim Min-Seok, Chung Sung-Chong. Integrated design methodology of ball-screw driven servomechanisms with discrete controllers. Part II: Formulation and synthesis of the integrated design. Mechatronics 2006;16(8):503–12. ISSN: 0957-4158.
[18] Zanasi R, Grossi F, Giuliani N. Dynamic modeling and control of a new automatic corking machine for threaded plastic caps. In: Proc. of IEEE 16th conference on emerging technologies & factory automation (ETFA); 2011. p. 1–8.
[19] Zanasi R, Grossi F. The POG technique for modelling multi-phase permanent magnet synchronous motors. In: 6th EUROSIM congress on modelling and simulation, Ljubljana; 9–13 September 2007.
[20] Zanasi R, Grossi F. Multi-phase synchronous motors: POG modeling and optimal shaping of the rotor flux. ELECTRIMACS 2008, Québec, Canada; June 2008.
[21] Grimme E. Krylov projection methods for model reduction. Ph.D. thesis, Coordinated Science Laboratory, University of Illinois at Urbana-Champaign; 1997.
[22] Zanasi R, Grossi F. Modelling hybrid automotive systems with the POG technique. J Asian Electric Vehicles 2010;8(1):1379–84.
[23] Khalil HK. Nonlinear systems. Third ed. Prentice Hall; 2002. ISBN: 0-13-067389-7.
[24] Gawthrop PJ. Bond graphs: a representation for mechatronic systems. Mechatronics 1991;1(2):127–56.
[25] Seo K, Fan Z, Hu J, Goodman ED, Rosenberg RC. Toward a unified and automated design methodology for multi-domain dynamic systems using bond graphs and genetic programming. Mechatronics 2003;13(89):851–85. ISSN: 0957-4158.
[26] Gawthrop PJ, Bevan GP. Bond-graph modeling. IEEE Control Syst Mag 2007;27(2):24,4.
[27] Breedveld PC. Multibond graph elements in physical systems theory. J Franklin Inst 1985;319(1–2):1–36.